

1 6.4.10.1 Disposal System Flow and Transport Modeling (BRAGFLO and NUTS)

2 In BRAGFLO, initial conditions ~~for the simulation of~~ *to simulate* the regulatory period are
3 consistent with the following:

- 4 **1. (1)** there are no gradients for flow in the far-field Salado;
- 5 **2. (2)** Salado far-field pore pressures are elevated above hydrostatic from the surface but
6 below lithostatic; and
- 7 **3. (3)** near the repository, excavation and waste emplacement results in partial drainage of
8 the DRZ, ~~and~~ subsequent evaporation of drained brine into mine air, and ~~then~~
9 removal from the modeled system by air exchanged to the surface.

10 The term “far-field” ~~used above~~ refers to the region that is not influenced by the ~~drainage of the~~
11 DRZ *drainage* mentioned in (3). For units above the Salado, initial pressures are ~~set to be~~
12 consistent with observed pore pressures or normal hydrostatic gradients (*Appendix PA, Section*
13 *4.2.2*).

14 Estimating the effects of drainage of the DRZ that occurs during the operational period,
15 (3) above, is not simple. For each vector sampled in LHS, the DOE estimates this by using
16 BRAGFLO to simulate a period of time representing disposal operations. This calculation is
17 called the start-up simulation and covers five years from $t = -5$ years to $t = 0$ years,
18 corresponding to the amount of time a typical panel is expected to be open during disposal
19 operations. Most of the initial parameters used during the regulatory period simulation ($t = 0$ to
20 $t = 10,000$ years) are also assigned for the start-up simulations, with some exceptions, ~~that are~~
21 described below.

22 The initial pressures in the Salado for the start-up simulation are ~~calculated~~ based on a sampled
23 pressure at the elevation of MB139 at the shaft and adjusted throughout the Salado and the DRZ
24 to account for changes in hydraulic head due to elevation change. This parameter is discussed in
25 Appendix *PA, Attachment PAR* (Parameter 26). ~~This~~ *The* adjustment assumes hydrostatic
26 equilibrium. The DRZ permeability is set at 10^{-17} square meters for the start-up simulation.
27 Based on observed changes in the DRZ, the DRZ porosity is adjusted upwards 0.0029 (0.29
28 percent) from the sampled value for intact, impure halite. Initial pressure for the start-up
29 simulation in the excavated regions is set to atmospheric. The shaft exists and is modeled as
30 unfilled with the same physical properties as the excavation.

31 For the start-up simulation, an initial water-table surface is specified within the Dewey Lake at
32 an elevation of 980 m (3,215 ft) above mean sea level. This elevation is consistent with
33 observations discussed in *Chapter 2, Section 2.2.1.4.2.1*. Above the water table, pressure is
34 maintained at one atmosphere, 0.101 megapascals; liquid saturations in these computational cells
35 are held constant at residual liquid saturation (Section 6.4.6.6, ~~Table 6-25~~ *Table 6-23*). Below the
36 water table, initial liquid saturations in all regions except the repository and shaft are 100
37 percent. Pressures are set consistent with a hydrostatic gradient below the water table within the
38 Dewey Lake, as well as in the Rustler, except for the Magenta and Culebra. *Initial pressures in*
39 *the Culebra and Magenta are set at 0.9141 and 0.9465 megapascals, respectively. These*

1 *values are based on fluid level and fluid density data collected from well C-2737, which is*
2 *located directly over the waste panels (Beauheim 2003).* ~~An initial pressure for the Culebra is~~
3 ~~set at 0.822 megapascals, based on fluid level and fluid density data collected at H-1, H-2B, H-3,~~
4 ~~H-4B, H-5B, H-6B, P-14, P-15, and P-17. An initial pressure of 0.917 megapascals is specified~~
5 ~~for the Magenta, calculated from fluid level and fluid density data from H-1, H-2A, H-3, H-4A,~~
6 ~~H-5A, and H-6A (Dotson 1996) Even though the natural properties of the units above the Salado~~
7 ~~vary considerably over the domain modeled by BRAGFLO, the BRAGFLO initial condition of~~
8 ~~constant pressure and constant properties for each layer is considered reasonable because the~~
9 ~~purpose of the BRAGFLO calculation with respect to these units is to calculate~~ the long-term
10 flux of brine from the borehole or shaft to each unit or to the surface. For this purpose, the
11 pressure and properties at the borehole or shaft are important, but details of regional hydraulic
12 head and unit properties are not.

13 For the start-up simulation, permeabilities of all units above the Salado are set to zero so that
14 flow cannot occur from these units into the shaft. This modeling assumption is adopted as a
15 simple method of accounting for the ~~existence of~~ effective liners in the shafts during disposal
16 operations.

17 ~~For the start-up simulation, n~~ No-flow boundary conditions are assigned in the BRAGFLO model
18 of the disposal system along all of the exterior boundaries of the computational mesh, except at
19 the far field boundaries of the Culebra and Magenta and the top of the model (that is, the ~~surface~~
20 ~~of the ground~~ *surface, Appendix PA, Section PA-4.2.10*). ~~These boundaries are 20 km from the~~
21 ~~edge of the Land Withdrawal Area boundary, as discussed in Section 6.4.2.1.~~ The ground
22 surface is maintained at atmospheric pressure. The boundaries of the Culebra and Magenta are
23 maintained at pressures of ~~0.822~~ *0.9141* megapascals and ~~0.954~~ *0.9465* megapascals,
24 respectively, corresponding to the initial pressure conditions used in the Culebra and Magenta.
25 The pressure in the Castile brine reservoir is set at its sampled value for the start-up simulation.

26 During the start-up simulation, fluid flow calculated by BRAGFLO from the Salado and the
27 DRZ into the excavated region simulates the effect of drainage into the repository during the
28 operational period. Following ~~the completion of~~ the start-up simulations, ~~specification of~~ initial
29 conditions ~~occurs~~ *are specified* for the regulatory period simulation. Boundary conditions for the
30 regulatory period simulation are the same as those for the start-up simulation.

31 The regulatory period simulation begins with conditions ~~specified~~ consistent with the sealing of
32 the repository by ~~construction of~~ shaft seals. Certain properties assigned for the start-up
33 simulation are changed to make model conditions consistent with the emplacement of waste and
34 completion of sealing. The liquid saturation in the waste-disposal region of the repository is set
35 at 0.015, which is a conservative value (Butcher 1996), and other areas of the excavation are
36 assigned zero liquid saturation (100 percent gas saturation) regardless of the quantity of brine
37 that may have flowed into the excavation during the start-up simulations. This is consistent with
38 the observed ability of circulating mine air to remove any inflowing brine by evaporation. The
39 entire repository is assigned an initial pressure of one atmosphere. Pressures and saturations in
40 model regions representing rock remain as they were ~~calculated to be~~ at the end of the start-up
41 simulation. Permeabilities of the units above the Salado are reset to the values specified ~~for them~~
42 as discussed in Section 6.4.6. The shaft is assigned properties for shaft seal materials discussed
43 in Section 6.4.4 *and Appendix PA, Section PA-4.2.6.* ~~The pressure in the shaft is set to one~~

1 atmosphere, and the liquid saturation of shaft materials is set to 1.0 except in asphalt, where
 2 liquid saturation is 0 percent. Waste is emplaced in the waste-disposal regions at a density of
 3 $1.171.63 \times 10^2 \text{ kg/m}^3$ for ferrous metals and $5.556.52 \times 10^1 \text{ kg/m}^3$ for biodegradable materials.
 4 and Other waste properties are assigned as discussed in Section 6.4.3.2. Panel closure
 5 properties discussed in Section 6.4.3.2 are assigned to the panel closure regions. Permeability in
 6 the DRZ is *sampled for each realization and* remains constant for the regulatory period
 7 simulation (see *Appendix PA, Attachment PAR*). Corrosion and biodegradation reactions that
 8 produce gas are modeled to begin at the start of the regulatory period simulation, and their rates
 9 depend on the sampled parameter values for the gas generation model (see Section 6.4.3.3) and
 10 the availability of brine. Modeling of creep consolidation through the use of the porosity surface
 11 also begins at this time (see Section 6.4.3.1).

12 6.4.10.2 Culebra Flow and Transport Modeling (*MODFLOW-2000* SECOFL2D, SECOTP2D)

13 Groundwater flow in the Culebra is computed at both a regional and local scale. Regional scale
 14 simulations are performed over a large domain using a computational grid that is coarser than the
 15 grid used for the local scale. The regional domain covers only a portion of the natural hydrologic
 16 system. A correct flow field can be calculated for any arbitrary part of a more extensive system
 17 if the transmissivity distribution and the values of hydraulic head assigned at the boundaries are
 18 representative of observed conditions. There is therefore considerable flexibility in choosing the
 19 locations of boundaries for the regional SECOFL2D model. *Two principal* Several factors were
 20 considered in *when* selecting these boundaries *for the MODFLOW-2000 model of the Culebra.*
 21 *First, model boundaries should coincide with natural groundwater divides where feasible, or*
 22 *be far enough from the area of most interest (the SECOTP2D transport domain) to have*
 23 *minimal influence in that area. Second, the model domain should encompass all features with*
 24 *the potential to affect Culebra water levels at the WIPP site (e.g., potash tailings ponds).* One
 25 side of the rectangular domain was aligned along a natural hydrologic feature, the axis of Nash
 26 Draw. The size of the model domain was selected such that the domain does not extend a great
 27 distance beyond the region of concentrated transmissivity and hydraulic head data but was large
 28 enough that the imposed boundary conditions would not have a large influence on the solution in
 29 the region of interest. The results of the regional scale simulations are used to interpolate
 30 boundary conditions at the local scale. This modeling approach allows the use of high resolution
 31 computational grids in the region of interest for computing radionuclide transport and the
 32 incorporation of a flow field representing a larger area.

33 *The modeling domain is approximately 22.3 km (14 mi) east-west by 30.6 km (19 mi) north-*
 34 *south, aligned with the compass directions (see Figure 6-17 in Section 6.4.6.2). This is the*
 35 *same as the domain used by LaVenue et al. (1990), except that the current domain extends*
 36 *1 km farther to the west. The modeling domain is discretized into 68,768 uniform 100-m ×*
 37 *100-m cells. The northern model boundary is slightly north of the end of Nash Draw, 12 km*
 38 *(7.5 mi) north of the northern WIPP site boundary. The eastern boundary lies in a low-*
 39 *transmissivity region that contributes little flow to the modeling domain. The southern*
 40 *boundary lies 12.2 km (7.6 mi) south of the southern WIPP site boundary, slightly over 1.7 km*
 41 *(1 mi) south of the southernmost well (H-9) and far enough from the WIPP site to have little*
 42 *effect on transport rates on the site. These boundaries are all assigned constant-head*
 43 *conditions based on head measurements made in model domain wells. The western model*
 44 *boundary passes through the IMC tailings pond due west of the WIPP site in Nash Draw.*

1 *However, a no-flow boundary (a flow line) is specified in the model from this tailings pond up*
2 *the axis of Nash Draw to the northeast, reflecting the concept that groundwater flows down*
3 *the axis of Nash Draw, forming a groundwater divide. Similarly, another no-flow boundary is*
4 *specified from the tailings pond down the axis of the southeastern arm of Nash Draw to the*
5 *southern model boundary, coinciding with a flow line in the regional modeling of Corbet and*
6 *Knupp (1996). Thus, the northwestern and southwestern corners of the modeling domain are*
7 *specified as inactive cells in MODFLOW-2000, leaving 53,769 active cells.* The regional
8 domain is approximately 13.67 miles by 18.64 miles (22 kilometers by 30 kilometers) and is
9 aligned with the axis of Nash Draw along a portion of the western boundary (see Figure 6-17 in
10 Section 6.4.6.2). Nash Draw is a highly conductive region that behaves hydraulically as a
11 groundwater divide (see Section 2.2.1.1). Therefore, that portion of the western boundary
12 oriented along Nash Draw is represented by a no-flow boundary. The remaining regional
13 boundary conditions are positioned to align with topographic highs or other geologic features
14 such as the San Simon Swale on the southeast boundary. Because of uncertainty in boundary
15 heads, the boundaries are positioned a large distance from the local problem domain (see Figure
16 6-18 in Section 6.4.6.2). This is done to reduce the influence of these boundary conditions on
17 the solution in the region of interest. Because boundary head values can be easily estimated
18 numerically during the calibration of transmissivity fields from existing well data, Dirichlet
19 (constant head) boundary conditions are used on these boundaries (see also the discussion in
20 Section 6.4.6.2).

21 Boundary conditions of the local domain are Dirichlet (constant head) and derived by
22 interpolating the solution of the regional domain. Because these boundary conditions are set by
23 interpolation and because the simulations are steady state, Dirichlet and Neuman (specified flux)
24 boundary conditions will provide essentially identical results, and specification of the type of
25 boundary condition is not important.

26 An initial estimate of the undisturbed head distribution is required to analyze transient well data
27 needed to generate the transmissivity fields (see Section 6.4.6.2 and Appendix TFIELD, Section
28 TFIELD.2.2.4). These data were obtained from hydrographs of the WIPP boreholes measured
29 prior to the excavation of the first shaft. The hydrographs depict hydraulic heads for up to 5
30 years preceding shaft excavations. The transmissivity field calibration process develops a set of
31 boundary heads for the regional domain that are consistent with hydrograph observations and the
32 transmissivity field generated.

33 Initial conditions are not required for the Culebra flow calculations because these are steady
34 state. Initial actinide concentrations in the transport simulations are assumed to be zero.

35 6.4.10.3 Initial and Boundary Conditions for Other Computational Models

36 In addition to BRAGFLO, ~~SECOFL2D~~ **MODFLOW-2000**, and SECOTP2D, several other codes
37 are used in performance assessment **PA** that require initial and boundary conditions. In general,
38 these codes are strongly coupled to BRAGFLO, analogous to the manner in which SECOTP2D
39 is coupled to ~~SECOFL2D~~ **MODFLOW-2000**. These additional codes are NUTS, PANEL, the
40 BRAGFLO direct brine release model (BRAGFLO_DBR), and CUTTINGS_S.

1 NUTS transports radionuclides through the BRAGFLO domain based on fluid flow
 2 characteristics as calculated by BRAGFLO and, therefore, does not need explicit definition of
 3 flow boundary conditions. As actinide transport is not of concern until the repository contains
 4 waste and is sealed, a start-up simulation is not executed with NUTS. Boundary conditions for
 5 advective transport are consistent with the boundary conditions assumed for fluid flow.
 6 Molecular transport boundary conditions for NUTS simulations consist of no diffusion or
 7 dispersion in the normal direction across far-field boundaries. Initial actinide concentrations are
 8 zero in all regions except the waste. Actinide concentrations in brine in the waste region *brine*
 9 are assigned as discussed in Section 6.4.3.5 (*Table 6-13* ~~Table 6-11~~).

10 PANEL is used to estimate the transport of radionuclides from the repository to the Culebra for
 11 the E1E2 scenario (*Appendix PA, Section PA-4.4*). PANEL assumes homogeneous mixing
 12 within a panel of the waste disposal region for determination of *to determine* a source term for
 13 radionuclides. PANEL is strongly coupled to BRAGFLO, in that the flux of liquid up the
 14 borehole *and* out of the separate panel in BRAGFLO is provided as the flux of liquid leaving the
 15 mixing volume in PANEL. Liquid leaving the mixing cell in PANEL is assumed to arrive at the
 16 Culebra, thereby maximizing the source of actinides to the Culebra.

17 Models for direct release to the surface are also strongly coupled to BRAGFLO. CUTTINGS_S
 18 (cuttings, cavings, and spall) and BRAGFLO (*for direct brine release*)_DBR acquire fluid
 19 pressure, fluid saturation, and other necessary quantities from the appropriate BRAGFLO
 20 disposal system model simulation. It is assumed in the direct release models that radionuclides,
 21 once entrained in drilling fluid, remain in the drillhole until they reach the surface. In other
 22 words, there is no interaction between drilling fluid and the formations between the repository
 23 and the surface. Boundary conditions in the direct brine release model are no-flow except for the
 24 sources and sinks of brine through borehole nodes and at the surface.

25 **6.4.11 Numerical Codes Used in Performance Assessment**

26 To evaluate scenario consequences for both undisturbed and disturbed performance, the DOE
 27 uses many computer codes to simulate relevant features of the disposal system. The flow of
 28 information and primary roles of the codes used are discussed in this section; *the mathematical*
 29 *models implemented by the codes are discussed in Appendix PA.* ~~detailed discussion of the~~
 30 ~~individual codes is reserved for appendices, which are referenced as appropriate.~~ Parameter
 31 values and disposal system conditions must be passed between codes several times in an
 32 assessment.

33 The codes are executed under the requirements of the SCMS), which creates and maintains a
 34 complete record of the input data and results of each calculation, *together along* with the exact
 35 codes used to create those results. For this application, ~~performance assessment~~ *PA* codes used in
 36 conjunction with LHS or random sampling were executed under the SCMS.

37 The major computer codes and the flow of information among them are illustrated in ~~Figure 6-25~~
 38 *Figure 6-24*. As discussed in Section 6.1.4 and indicated in ~~Figure 6-25~~ *Figure 6-24*, some of
 39 these codes are used to calculate reference conditions for deterministic futures associated with
 40 the parameters in x_{su} (Equation 6.4b [Section 6.1.2]) and their associated uncertainty
 41 characterized by distributions D_{su} (Equation 6.6b [Section 6.1.2]). The results of these codes are
 42 then used in the construction of *constructing* the consequences of probabilistic futures. There

1 are three major steps in evaluating scenario consequences for deterministic futures:
 2 (1) ~~preparation of~~ *preparing* input from submodels executed independent of LHS (for example,
 3 SANTOS, *PEST*, *GRASP-INV*), (2) LHS of the variables x_{su} in the ~~performance assessment~~ *PA*
 4 parameter database, and (3) ~~execution of~~ *executing* the sampling-dependent ~~performance~~
 5 ~~assessment~~ *PA* codes (those within the deterministic futures box indicated by dashed lines in
 6 ~~Figure 6-25~~ *Figure 6-24*).

7 Some ~~performance assessment~~ *PA* codes are used to calculate probabilistic futures; that is, future
 8 events that occur randomly in time and space, and uncertainty ~~in~~ *of* associated parameters in x_{st}
 9 (Equation 6.4a [Section 6.1.2]) and ~~their uncertainty~~ characterized by distributions in D_{su}
 10 (Equation 6.6a [Section 6.1.2]). There are two major steps in evaluating scenario consequences
 11 for probabilistic futures: (1) random sampling of the parameter database, and (2) ~~execution of~~
 12 *executing* the codes.

13 ~~Figure 6-25~~ *Figure 6-24* indicates only those codes that perform the bulk of the computational
 14 effort related to simulating the significant physical processes occurring within the disposal
 15 system. In addition to these codes, a variety of additional codes are used in this ~~performance~~
 16 ~~assessment~~ *PA*. These additional codes are ~~used for the transfer of data between codes,~~
 17 ~~preparation of~~ *prepare* input files, model output processing, and *perform* similar tasks. These
 18 codes are also executed within the SCMS.

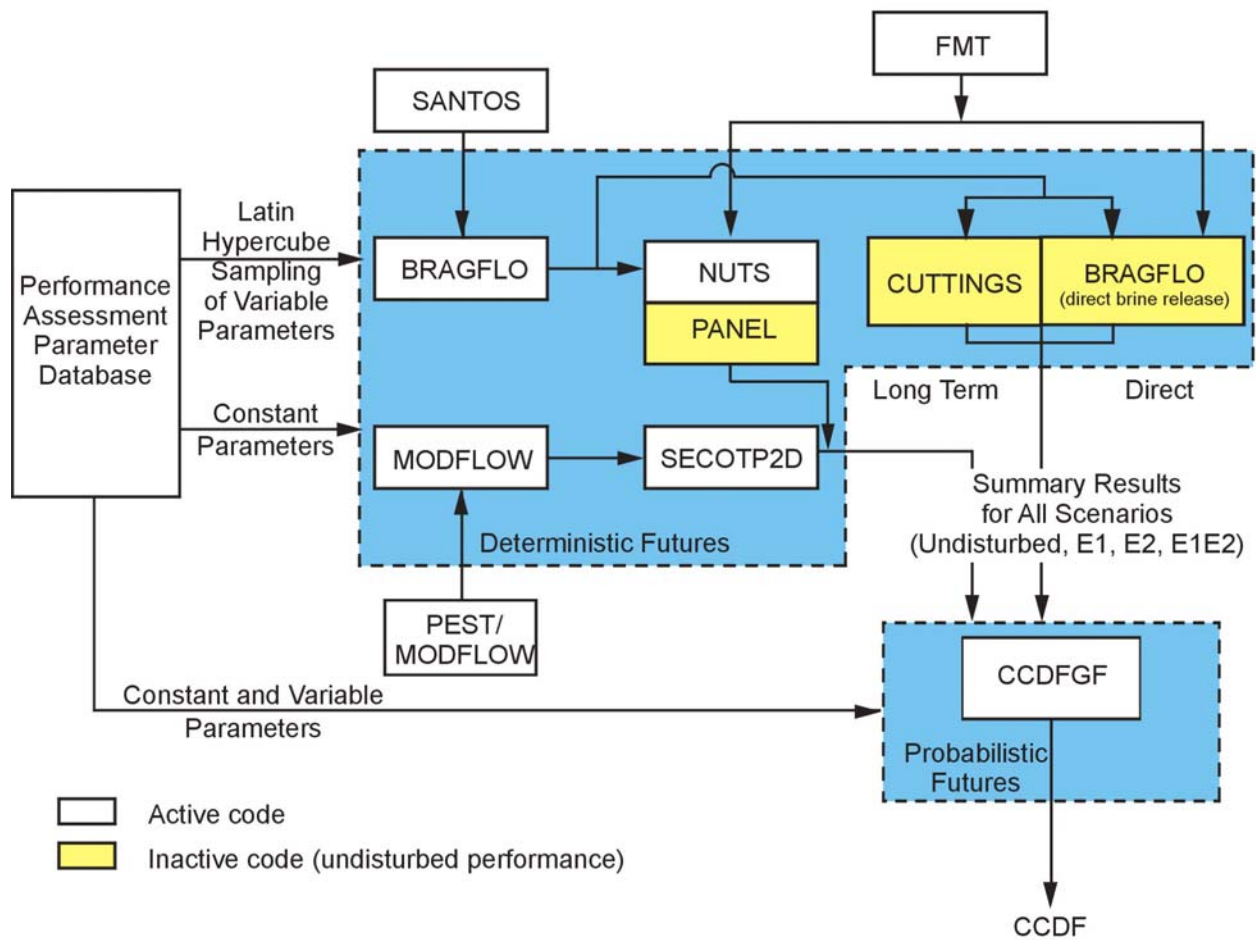
19 Because these additional codes are not expressly used ~~for simulation of~~ *to simulate* physical
 20 processes, they have been omitted from discussion here and on ~~Figure 6-25~~ *Figure 6-24* for
 21 clarity. A comprehensive description of the coupling of codes used in this ~~performance~~
 22 ~~assessment~~ *PA* is provided in *Appendix PA*. ~~Appendix CODELINK (see Table CODELINK-1).~~

23 ~~Figure 6-26~~ *Figure 6-25* shows an alternative method of visualizing how the various PA codes
 24 relate to each other and to the estimation of scenario consequences. This figure ~~represents~~ *shows*
 25 a vertical cross section of the disposal system, associating the major codes with the particular
 26 components of the system each code simulates. As shown in the figure, BRAGFLO, SANTOS,
 27 NUTS, and PANEL address the Salado. *PEST*, *GRASP-INV*, *SECOFL2D-MODFLOW-2000*,
 28 and *SECOTP2D* address the Culebra. *CUTTINGS_S*, BRAGFLO (*direct brine release*)-*DBR*,
 29 *DRSPALL*, and PANEL address the immediate consequences of inadvertent human intrusion
 30 through one or more exploratory boreholes. Combined, Figures ~~6-25~~ *6-24* and ~~6-25~~ *6-25* illustrate
 31 the flow of information through major ~~performance assessment~~ *PA* codes and the relationship
 32 between the codes and the physical system being simulated.

33 The parameter database is the initial element in the ~~performance assessment~~ *PA* process. The
 34 database includes the parameters used in ~~performance assessment~~ *PA* codes that pertain to the
 35 technical aspects of disposal system performance. Parameters pertaining only to the execution of
 36 the codes (for example, convergence criteria for Newton-Raphson numerical solvers) are
 37 generally not included in the database, but are recorded in input files and ~~are~~ traceable through
 38 the SCMS. The ~~p~~ parameters in the database fall into two categories: those that are assigned
 39 fixed values, and those that are uncertain and are therefore assigned a range of values according
 40 to a CDF.

41 Vectors (sets) of parameter values are created from the uncertain variables in the database by
 42 LHS of each variable for the *a* set of simulations *in the PA*. ~~comprising a performance~~

1 assessment of the system. In this performance assessment PA, 57 64 parameters are sampled
 2 using LHS, and 100 vectors are assembled in each replicate (see Section 6.5). The values
 3 assigned to each sampled parameter in each of the vectors in this performance assessment PA are
 4 included in Appendix PA, Attachment PAR IRES (Section IRES.1). Each of the fixed
 5 parameter values from the database and a vector of sampled parameter values are combined to
 6 form a realization (a set of input parameters). Each realization is then propagated through the
 7 performance assessment PA codes within the dashed lines shown in Figure 6-25 Figure 6-24.
 8 The assessment of Assessing each realization requires that the codes shown in Figure 6-25
 9 Figure 6-24 for deterministic futures be executed under four code sequence configurations, one
 10 each for the undisturbed performance scenario (E0), the E1 scenario, the E2 scenario, and the
 11 E1E2 scenario.



12
 13 **Figure 6-246-25. Major Codes, Code Linkages, and Flow of Numerical Information in**
 14 **WIPP Performance Assessment PA**

15 Each intrusion scenario may occur with or without mining. The techniques used for each
 16 scenario are described in Section 6.4.13.

1 As shown in *Figure 6-25*, information for some of the major codes comes from the following
2 additional sources: the SANTOS, *PEST*, *DRSPALL* GRASP-INV, and FMT codes.

3 The SANTOS code develops the porosity surface, describing porosity as a function of time and
4 pressure; this information is used in the BRAGFLO code (see *Appendix PA, Section PA-4.2 and*
5 *Attachment PORSURF* Appendices BRAGFLO, Section 4.11, and PORSURF, Section
6 PORSURF.1). *PEST is coupled with MODFLO-2000 to* GRASP-INV calculates numerous
7 possible and equally likely Culebra transmissivity fields; these transmissivity fields are used
8 in the ~~SECOFL2D~~ *MODFLOW-2000* code (see Appendix *PA, Attachment* TFIELD, Section
9 TFIELD.4, and Appendix CODELINK, Section CODELINK.6.4). FMT is used to calculate
10 solubility parameters that were entered into the parameter database. These parameters, as well as
11 sampled solubility distribution parameters, were used to calculate solubilities for the
12 performance assessment *PA*. Actinide solubility in the repository is used by the codes NUTS and
13 PANEL. *DRSPALL calculates the volume of solid material that could be removed from the*
14 *repository by spillings for a set of initial pressure conditions and uncertain parameters. The*
15 *code CUTTINGS_S uses the DRSPALL results to determine the volume removed by spillings*
16 *for intrusions at different times and locations.*

17 The performance assessment *PA* codes are executed sequentially. Following LHS, BRAGFLO is
18 the first major code executed. Notice that the code BRAGFLO is listed twice in this sequence.
19 BRAGFLO is used in two applications for performance assessment *PA*. In the first application,
20 BRAGFLO calculates the overall movement of gas and brine in the repository and from the
21 Castile to the surface; this movement forms the basis for estimating radionuclide releases to the
22 accessible environment (Appendix *PA Sections 4.2 and 6.7* BRAGFLO, Sections 4.1 through
23 4.9). BRAGFLO also contains subsystem models for estimating gas generation in the repository,
24 disposal room closure and consolidation, and interbed fracturing (Appendix *PA, Section PA-4.2*
25 BRAGFLO, Sections 4.10 through 4.13). BRAGFLO does not calculate the movement of
26 radionuclides. The second application of BRAGFLO is discussed below.

27 NUTS calculates the overall movement and decay of radionuclides in the repository and disposal
28 system. NUTS uses the same geometry as BRAGFLO, the brine and gas flow fields calculated
29 by BRAGFLO, and the radionuclide source concentrations (solubilities) in the repository defined
30 by the actinide source term models. In simulations of the E1 scenario, NUTS also tracks brine
31 originating in the Castile brine reservoir, including the fraction of Castile brine that has flowed
32 out from the borehole and into the waste in the repository. See Appendix *PA, Section*
33 *PA-4.3* NUTS (Section 4) for additional information on the use of NUTS in performance
34 assessment *PA*. PANEL calculates actinide source term to the Culebra for the E1E2 scenario, as
35 discussed in Section 6.4.13.5. PANEL is described in detail in Appendix *PA, Section PA-4.4.*
36 ~~NEL.~~

37 In all scenarios, the quantity of brine flowing up the shafts or a degraded exploratory borehole to
38 the Culebra is calculated by BRAGFLO, and the concentration of radionuclides in that brine,
39 calculated by NUTS or PANEL, is used to determine the quantity of radionuclides released to
40 the Culebra.

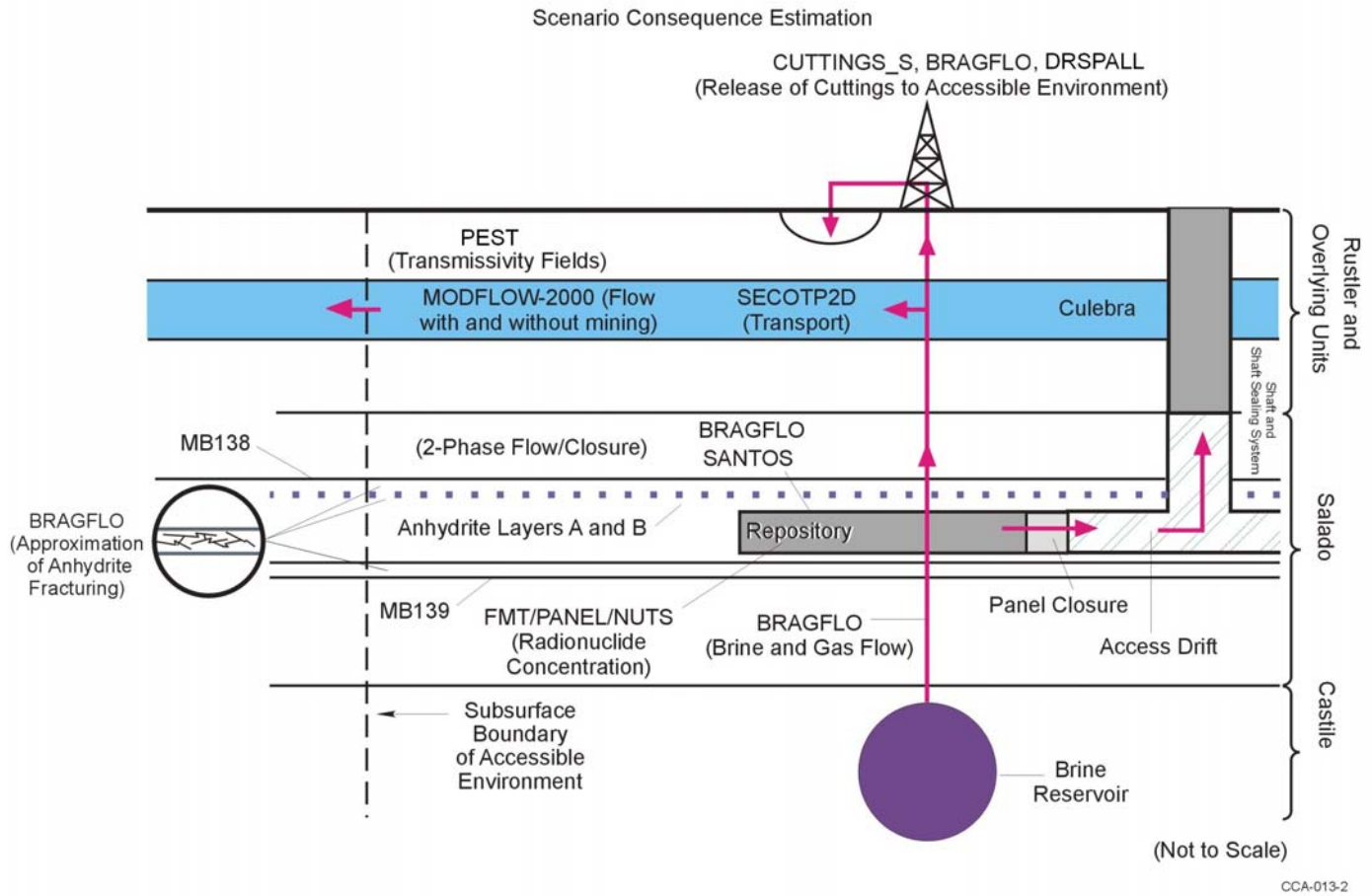
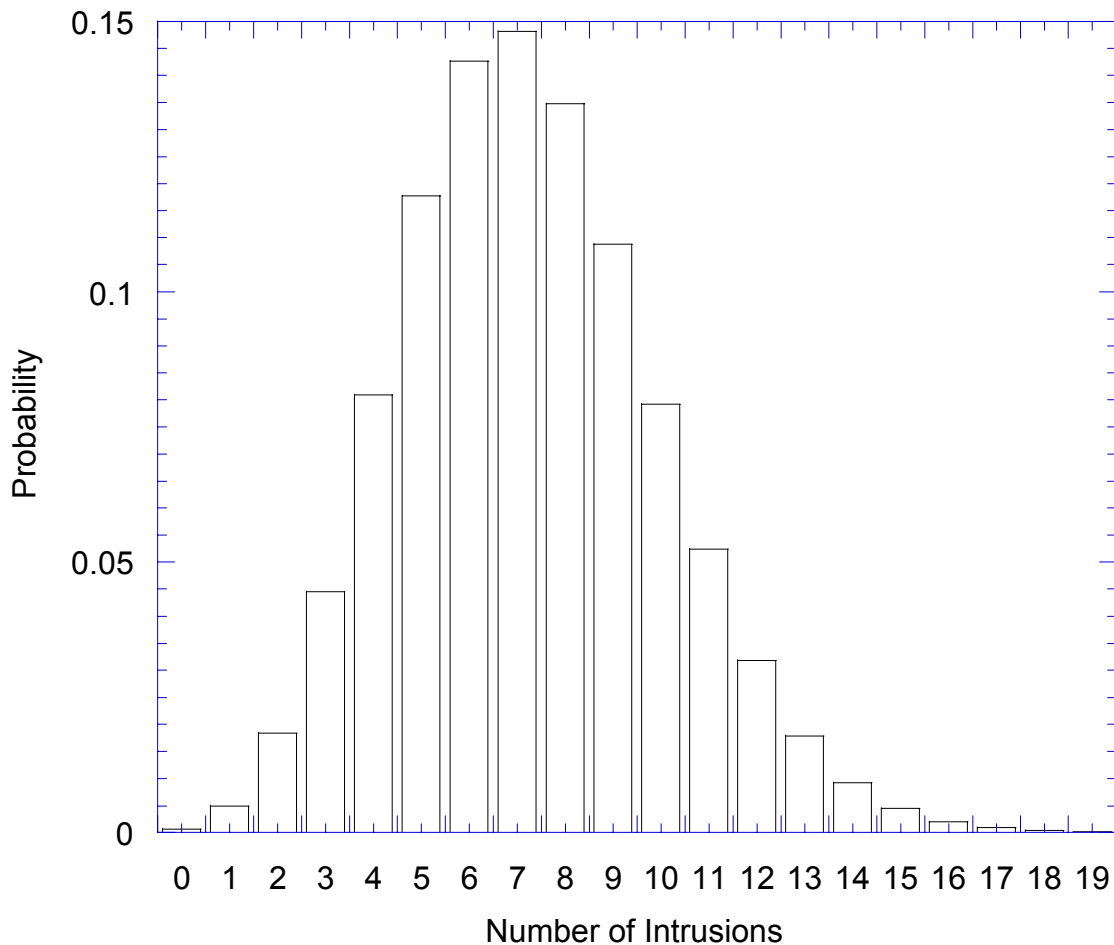


Figure 6-256-26. Schematic Side View of the Disposal System Associating Performance Assessment PA Codes with the Components of the Disposal System Each Code Simulates

March 2004

6-158

DOE/WIPP 2004-3231



1
2 **Figure 6-266-27. Probability of Intrusions in 10,000 Years with Active Institutional**
3 **Control**

4 CUTTINGS_S and BRAGFLO_DBR (*direct brine release*) are used to evaluate the immediate
5 consequences of inadvertent human intrusion through exploratory drilling. Solid material and
6 brine may be transported to the surface in the drilling fluid. After pressure in the repository is
7 relieved through the first borehole, subsequent boreholes may release less material to the surface.
8 CUTTINGS_S calculates the quantity of solid material transported to the accessible environment
9 at the surface during the drilling activities. This includes material removed directly from the
10 borehole (cuttings), together along with cavings and spallings. The code is discussed in
11 Appendix PA, Section PA-4.5 CUTTINGS. BRAGFLO_DBR (*direct brine release*) is used to
12 calculate the quantity of brine transported up the borehole to the surface.

13 SECOFL2D-MODFLOW-2000 and SECOTP2D together calculate the detailed movement of
14 radionuclides in the Culebra that occurs if radionuclides are introduced by flow up the shafts or
15 through a degraded exploratory borehole. SECOFL2D MODFLOW-2000 calculates regional
16 Culebra flow fields using an assumption that flow occurs in a single-porosity medium.
17 SECOFL2D MODFLOW-2000 uses the transmissivity fields calculated by calibrated using
18 PEST GRASP INV (one field in each simulation). SECOTP2D calculates radionuclide transport

1 in a double-porosity medium, accounting for advection in fractures, matrix diffusion, retardation,
2 and decay, as described in Section 6.4.6.2. ~~SECOFL2D~~ *MODFLOW-2000 and SECOTP2D* ~~is~~
3 *are* discussed in Appendix *PA, Section PA-48 and PA-49, respectively*. ~~SECOFL2D;~~
4 ~~SECOTP2D is discussed in Appendix SECOTP2D.~~ The NUTS and PANEL codes calculate the
5 actinide source term to the Culebra.

6 The computer code CCDFGF is used to (1) determine random sequences of future events that
7 may occur over the next 10,000 years at the WIPP site; (2) estimate the radionuclide releases
8 resulting ~~for~~ *from* these random sequences of future events using the results of ~~the~~ calculations
9 described thus far ~~in Section 6.4;~~ and (3) construct a CCDF for each realization. The manner in
10 which CCDFGF determines random sequences of future events is the subject of Section 6.4.12.

11 ~~The estimation of~~ *Estimating* consequences and ~~construction of~~ *constructing* a CCDF for these
12 sequences of future events is the subject of Section 6.4.13.

13 *6.4.12 Sequences of Future Events*

14 For this application, sequences of future events that may occur are determined using a random
15 sampling procedure described in Appendix *PA, Section PA-3.0* ~~CCDFGF (Section 3.2)~~. A
16 general description of the technique is presented in this section.

17 The incorporation of stochastic uncertainty in the ~~performance assessment~~ *PA* is based on
18 repeatedly generating independent sequences of events that may occur at the WIPP over the next
19 10,000 years. Each 10,000-year sequence is generated by randomly sampling six parameters that
20 repeatedly characterize stochastic uncertainty about future events. These parameters include (1)
21 the interval of time between drilling intrusions (which yields both the number and time of
22 intrusions), (2) the location of each drilling intrusion, (3) the activity of the waste penetrated by
23 each drilling intrusion, (4) the plug configuration in the intrusion borehole, (5) the penetration of
24 a Castile brine reservoir, and (6) the occurrence of mining. Probability distribution functions are
25 assigned to each of these six parameters and are discussed in the following sections. Random
26 sampling from these distributions ~~is used to generate~~ *s* 10,000 equally likely, independent futures
27 ~~for~~ *of* the WIPP for each realization executed and CCDF constructed. The computer code
28 CCDFGF (Appendix *PA* ~~CCDFGF, Sections 3 and PA-6.0.2~~) ~~is used to randomly sample~~
29 sequences of future events, ~~constructs~~ *s* consequences of these sequences, and ~~assembles~~ *s* CCDFs.
30 As described in Section 6.4.13, normalized integrated radionuclide releases to the accessible
31 environment are estimated for each history using the consequence modeling system.

32 The probability assigned to the occurrence of certain ~~in the~~ future events at the WIPP site is
33 affected by regulatory guidance and ~~by~~ *DOE* actions taken ~~by the DOE~~ to deter activities
34 detrimental to WIPP performance. Active and passive institutional controls are discussed
35 extensively in Chapter 7.0. A summary of their use in ~~performance assessment~~ *PA* ~~begins the~~
36 ~~discussion~~ *is* in this section.

37 *6.4.12.1 Active and Passive Institutional Controls in Performance Assessment*

38 Active institutional controls and passive institutional controls will be implemented at the WIPP
39 site to deter human activity ~~that may be detrimental to the performance of the repository~~
40 *performance*. Active institutional controls and passive institutional controls are described in

1 detail in Chapter 7.0 and in appendices referenced in Chapter 7.0. In this section, the impact of
 2 active institutional controls and passive institutional controls ~~to~~ *on* performance assessment *PA* is
 3 described.

4 Active institutional controls will be implemented at the WIPP after final facility closure to
 5 control ~~access to the site~~ *access* and ~~to ensure that activities detrimental to the performance of the~~
 6 disposal system *performance* do not occur within the controlled area. The active institutional
 7 controls will preclude human intrusion in the disposal system. A limitation for considering the
 8 effectiveness of active institutional controls in performance assessment *PA* is established in
 9 40 CFR Part 191. That limitation is 100 years. Because of the nature of the ~~system of active~~
 10 institutional controls to be implemented and regulatory restrictions, ~~it is assumed in the~~
 11 performance assessment *PA* that *assumes* there ~~can be~~ *are* no inadvertent human intrusions or
 12 mining in the controlled area for 100 years following repository closure.

13 Passive institutional controls ~~have a function in deterring~~ inadvertent human intrusion into the
 14 disposal system in performance assessment *PA*. ~~While~~ *Only* minimal assumptions were made
 15 about future society for the purposes of *when* designing the passive institutional controls to
 16 comply with the assurance requirements. ~~, more detailed assumptions are made in order to~~
 17 ~~quantify the effectiveness of passive institutional controls for performance assessment.~~ The
 18 preamble to 40 CFR Part 194 limits any credit for passive institutional controls in deterring
 19 human intrusion to 700 years after disposal (EPA 1996a, 61 FR 5231). *Although the DOE*
 20 *originally included credit for passive institutional controls in PA, the CRA-2004 PA does not*
 21 *include such credit. The EPA directed DOE not to take credit for passive institutional controls*
 22 *in the CCA during the certification (EPA 1998, 194.VIII.D.3).* This suggested time limit is
 23 important in quantifying the effectiveness of passive institutional controls for performance
 24 assessment purposes. ~~Because active institutional controls are effective for the first 100 years,~~
 25 ~~passive institutional controls are effective for the period of time from 100 to 700 years, or a~~
 26 ~~duration of 600 years.~~

27 ~~The effectiveness of passive institutional controls is implemented in performance assessment by~~
 28 ~~reducing the rate of human intrusion and mining by a factor that estimates the effectiveness of~~
 29 ~~passive institutional controls. As discussed in Appendix EPIC, passive institutional controls are~~
 30 ~~assumed to be 0.99 effective, meaning that the rate of deep drilling and mining for the 600-year~~
 31 ~~duration of passive institutional controls is a factor of 0.01 times the respective rates for the~~
 32 ~~uncontrolled period following 700 years. Because passive institutional controls are designed to~~
 33 ~~protect the controlled area, this reduction factor is applied to the entire controlled area.~~

34 6.4.12.2 Number and Time of Drilling Intrusions

35 The number of drilling intrusions associated with each 10,000-year history is based on 40 CFR
 36 § 194.33(b)(2) and § 194.33(b)(3):

37 In performance assessments, drilling shall be assumed to occur in the Delaware Basin at random
 38 intervals in time and space during the regulatory time frame. [40 CFR 194.33(b)(2)]

39 The frequency of deep drilling shall be calculated in the following manner:

1 (i) Identify deep drilling that has occurred for each resource in the Delaware Basin over the past
2 100 years prior to the time at which a compliance application is prepared.

3 (ii) The total rate of deep drilling shall be the sum of the rates of deep drilling for each resource.
4 [40 CFR 194.33(b)(3)]

5 The DOE's implementation of these criteria is described in this and the following sections.

6 Mathematically, events that are random in time can be described as following a Poisson process
7 that can be written in a simple form as

$$8 \quad P[E_n(\Delta t)] = \frac{[\lambda(\Delta t)]^n}{n!} e^{-\lambda\Delta t}, \quad (136.17)$$

9 where $p[E_n(\Delta t)]$ is the probability (p) that some number (n , an integer) of events (E) will occur in
10 a time interval (Δt) given a rate constant λ with units of events per time.

11 Inadvertent human intrusions may occur at any time between 100 years and 10,000 years after
12 the decommissioning of the facility. Both the number and time of intrusions are determined
13 sequentially by sampling from a CDF derived from the Poisson model that probabilistically
14 describes the time period ~~that elapses~~ *elapsing* between an intrusion at a fixed time and the next
15 intrusion. The time interval to the next intrusion following an intrusion may vary from 0 years to
16 greater than 9,900 years, with a probability determined by the rate constant λ . The rate constant
17 is derived from the drilling rate established for the Delaware Basin and the area of the waste
18 disposal region, 0.126 km² (0.049 mi²). The drilling rate used in this analysis was ~~52.5~~ *46.8*
19 boreholes per square kilometer per 10,000 years. As discussed in Appendix *DATA, Attachment*
20 *A-DEL* (Section ~~DEL-7.4~~), this rate is based on a review of past and present drilling activity in
21 the Delaware Basin. The rate constant λ is assigned different values for ~~two~~ *three* time periods.
22 While active institutional controls are effective, it is equal to zero; *after active institutional*
23 *controls cease, λ is assigned to 52.5 boreholes per square kilometer per 10,000 years.*, and
24 while passive institutional controls are effective, it is two orders of magnitude lower than during
25 the uncontrolled period (700 to 10,000 years).

26 ~~The CDF for intrusion times while passive institutional controls are effective is called the passive~~
27 ~~institutional controls CDF. The CDF for intrusion times after passive institutional controls may~~
28 ~~no longer be considered effective is called the post-passive institutional controls CDF. Sequences~~
29 ~~of future deep drilling events are constructed as follows. The passive institutional controls CDF~~
30 ~~is sampled to determine whether an intrusion occurs while passive institutional controls are~~
31 ~~effective. If the sampled time is greater than 600 years, zero intrusions occur before 700 years.~~
32 ~~If the time is less than 600 years, the passive institutional controls CDF is sampled again to~~
33 ~~determine whether a second intrusion occurs in the interval between the time of the first intrusion~~
34 ~~and 700 years. This procedure continues until a time of intrusion greater than 700 years is~~
35 ~~determined.~~

36 Intrusions times after 700 years are determined by *random* sampling. ~~the post-passive~~
37 ~~institutional controls CDF. If the sampled time is greater than 9,390 years (7100 + 9,390 =~~
38 ~~10,000), no intrusions occur between 7100 and 10,000 years. If the sampled time is less than~~

1 9,9300 years, an intrusion occurs at 7100 years plus the sampled time. The post-passive-active
 2 institutional controls CDF is sampled iteratively to determine whether intrusions occur in the
 3 time interval between the last intrusion and 10,000 years until an intrusion is determined to occur
 4 after 10,000 years.

5 Evaluation of the Poisson process for a specified rate constant and time interval yields the
 6 probability of occurrence of specified numbers of intrusions. Using a different rate constant for
 7 100 years of active institutional controls, 600 years of passive institutional controls, and 9300
 8 years of uncontrolled activity, the most likely number of intrusions into the waste disposal region
 9 during 10,000 years is five, occurring with a probability of 0.1715. Zero intrusions occur with a
 10 probability of 0.0041. The largest number of intrusions that occur with a probability greater than
 11 10^{-3} per 10,000 years (and which therefore can contribute to releases for comparison with the
 12 quantitative release limits) is 14, occurring with a probability of 0.0011. Probabilities for other
 13 numbers of intrusions within 10,000 years are given in Table 6-28. These probabilities are
 14 shown as a histogram in Figure 6-27.

15 *The most likely number of intrusions into the waste disposal region during 10,000 years is*
 16 *seven, with a probability of 0.1482. Zero intrusions occur with a probability of 0.0007. The*
 17 *largest number of intrusions that occur with a probability greater than 10^{-3} per 10,000 years*
 18 *(and which can contribute to releases for comparison with the quantitative release limits) is*
 19 *16, occurring with a probability of 0.0020. Probabilities for other numbers of intrusions*
 20 *within 10,000 years are given in Table 6-30. These probabilities are shown as a histogram in*
 21 *Figure 6-26.*

22 6.4.12.3 Location of Intrusion Boreholes

23 Drilling events are assumed to be random in time and space, and the location of each intrusion
 24 borehole within the waste disposal region is sampled randomly. This is done in the analysis by
 25 discretizing a plan view of the area within the passive institutional control berms (see *CCA*
 26 Appendix PIC, Section VIII) into 144 separate regions and requiring each intruding borehole to
 27 penetrate one, and only one, *a single* region (Figure 6-28 *Figure 6-27*). The probability of
 28 intersecting each location is equal to 1/144 (about 0.00694), and slight variations in the size of
 29 regions are disregarded as unimportant.

30 Each of the 144 regions contains both excavated and unexcavated areas at the repository horizon.
 31 A borehole penetration of a region has an approximately 20 percent chance of intruding
 32 excavations and *an* approximately 80 percent chance of passing through unexcavated Salado (*see*
 33 *Appendix PA, Section PA-3.4*). The berm area and the proportion of excavated to unexcavated
 34 regions at the repository horizon are important in the Castile brine reservoir model, as discussed
 35 in Section 6.4.12.6.

36 Boreholes that penetrate excavations may penetrate *either* CH-TRU waste *or* RH-TRU waste, *or*
 37 *panel closures that contain no waste*. For long-term releases and direct brine releases, all
 38 penetrations into excavations are treated as if CH-TRU waste is penetrated, and the RH-TRU
 39 waste inventory is averaged into the CH-TRU waste inventory for source-term determination.
 40 For cuttings and cavings direct releases, there is an approximately 12 percent chance that RH-
 41 TRU waste canisters are penetrated and an 88 percent chance that CH-TRU waste is penetrated,

1 **Table 6-306-28. Probabilities of Different Numbers of Intrusions into the Waste Disposal**
 2 **Region (for 100 years of active institutional control, ~~600 years of passive institutional~~**
 3 **~~control,~~ and 9,9300 years of uncontrolled activity)**

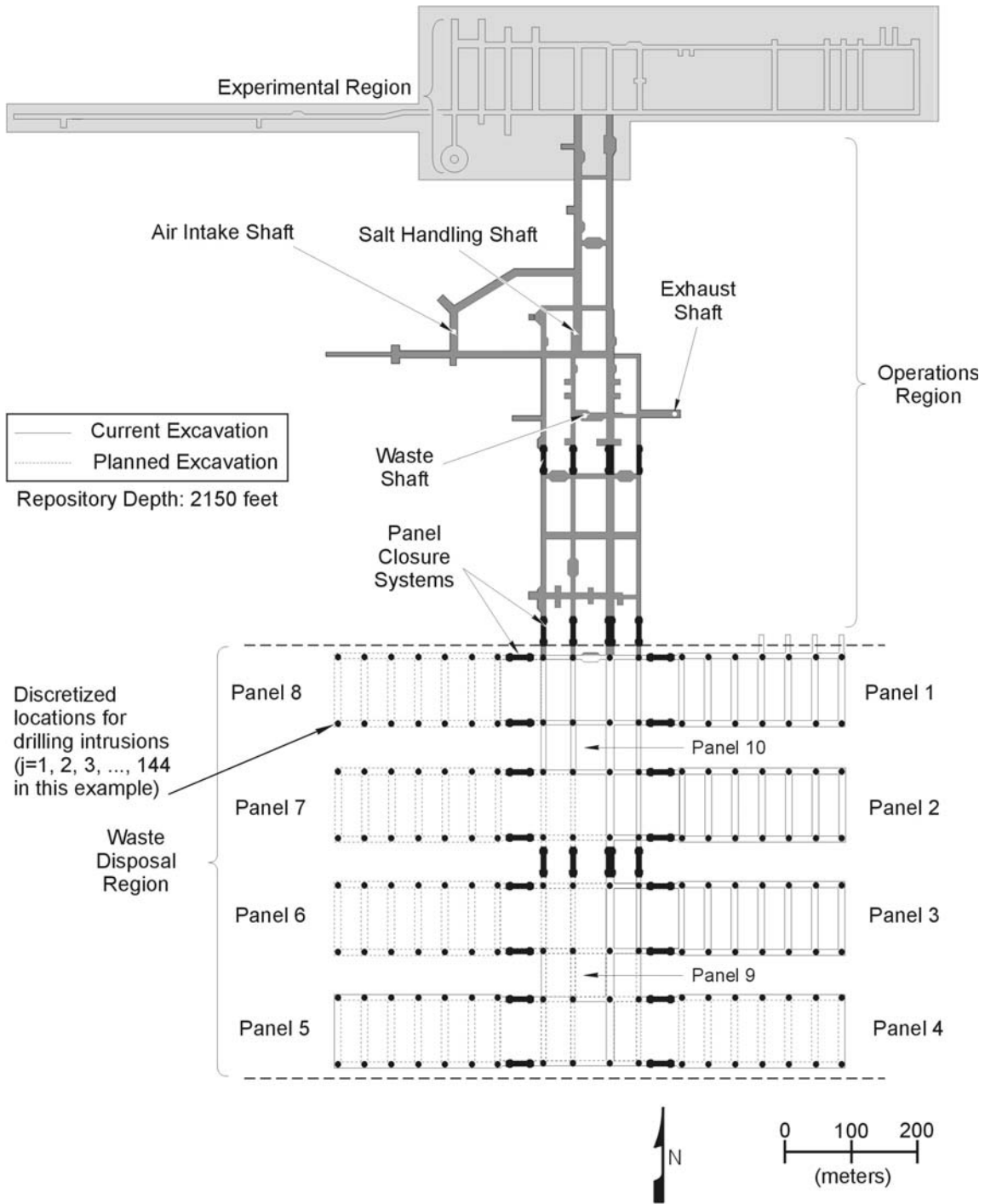
Number of Intrusions	Probability of Occurrence
0	0.000741
1	0.0050227
2	0.0183622
3	0.04451138
4	0.08091562
5	0.11771715
6	0.14261570
7	0.14821231
8	0.13480845
9	0.10890516
10	0.07920283
11	0.05240141
12	0.03180065
13	0.01780027
14	0.00920011
15	0.004504
16	0.0020
17	0.0009
18	0.0004
19	0.0001

4 corresponding to the relative plan-view areas of each waste type (*see Appendix PA, Section*
 5 *PA-3.7*). For cuttings and cavings direct releases, the small area of the panel closures is treated
 6 as CH-TRU waste and is included in the CH-TRU waste probability. Because of the low
 7 permeability of the region surrounding each RH-TRU waste canister, intrusions into RH-TRU
 8 waste are not assumed to produce spillings releases *or direct brine releases*. ~~Intrusions resulting~~
 9 ~~in spillings releases are treated as CH-TRU waste for the source term determination.~~

10 6.4.12.4 Activity of the Intersected Waste

11 Containers of waste shipped to the WIPP will contain quantities of radionuclides that will vary
 12 from container to container. Radioactivity may vary by several orders of magnitude from those
 13 waste containers with the largest quantities of radionuclides to those with the smallest.

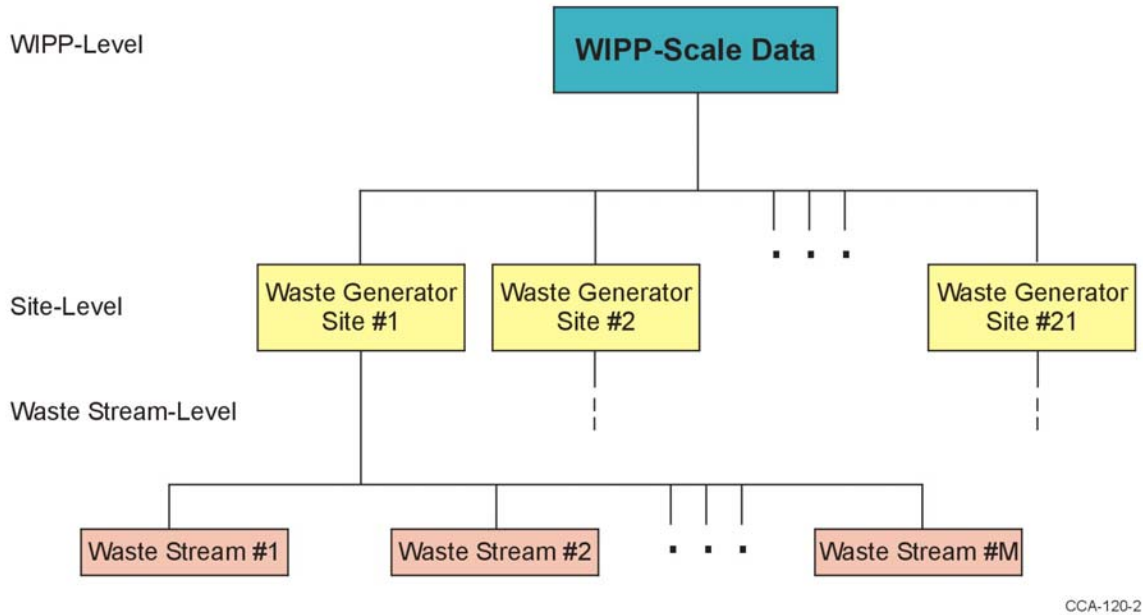
14 Information about waste radioactivity has been compiled at several different levels (~~Figure 6-29~~
 15 *Figure 6-28*). The waste-stream level includes information about waste activities from different
 16 processes at the generator sites that create TRU waste. At this level, a separate waste stream



CCA-014-2

1

2 **Figure 6-276-28. Discretized Locations for Random Intrusion by an Exploratory Borehole**

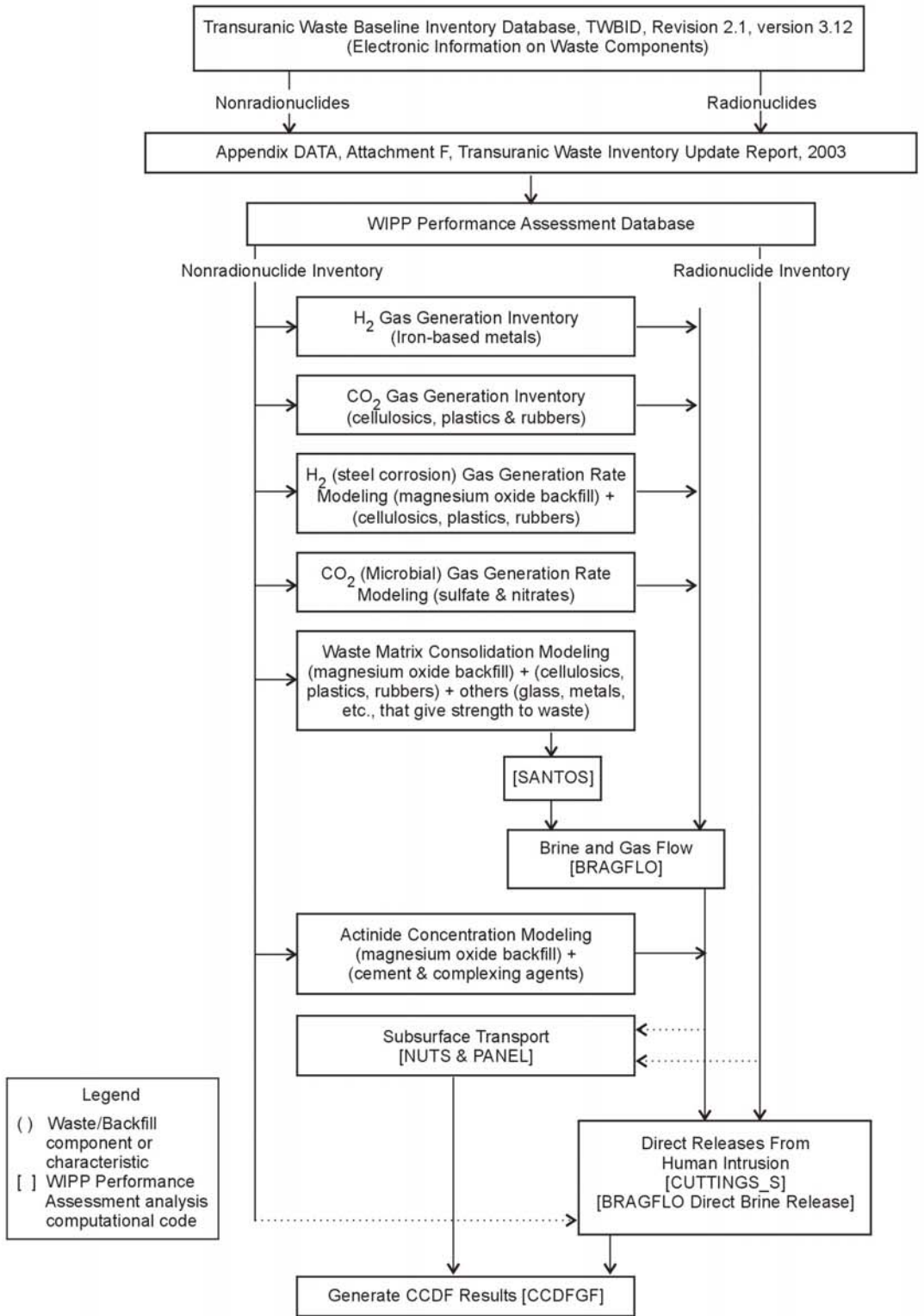


CCA-120-2

1
2 **Figure 6-286-29. Levels of Information Available in the TWBID**

3 characteristic is maintained for RH-TRU. In total, there are approximately 779 970 CH- and
 4 RH-TRU waste streams, of which 693 569 are CH-TRU. Because the RH-TRU is approximately
 5 one percent (actually 1.5 percent) of the total EPA units (not activity) of CH-TRU waste, all the
 6 RH-TRU waste was grouped (binned) together into one equivalent or average (WIPP-scale) RH-
 7 TRU waste stream. It is assumed that variability in this small fraction is *assumed to be*
 8 negligible. The waste-generator site level includes information integrated over the scale of a
 9 generator site. There are 27 24 generator sites identified for the WIPP (see Chapter Section
 10 4.1.2). The WIPP-scale level includes integrated information about all waste destined for the
 11 WIPP, including CH- and RH-TRU. Data are present for existing waste and estimates have been
 12 *were* made for future (to-be-generated) waste. The integration of waste data with the
 13 performance assessment PA is illustrated in Figure 6-30 *Figure 6-29. In the CCA, this*
 14 *information was* is compiled for the WIPP from the Transuranic Waste Baseline Inventory
 15 Database (TWBID), an electronic version of information present in the Transuranic Waste
 16 Baseline Inventory Report (TWBIR), Rev. 3, (see CCA Appendix BIR). *New information*
 17 *concerning waste inventory has been included in PA for emplaced, stored, and projected*
 18 *waste. The new information is discussed in Chapter 4 and Appendix TRU WASTE (see also*
 19 *Appendix DATA, Section 7.0, Attachment F).*

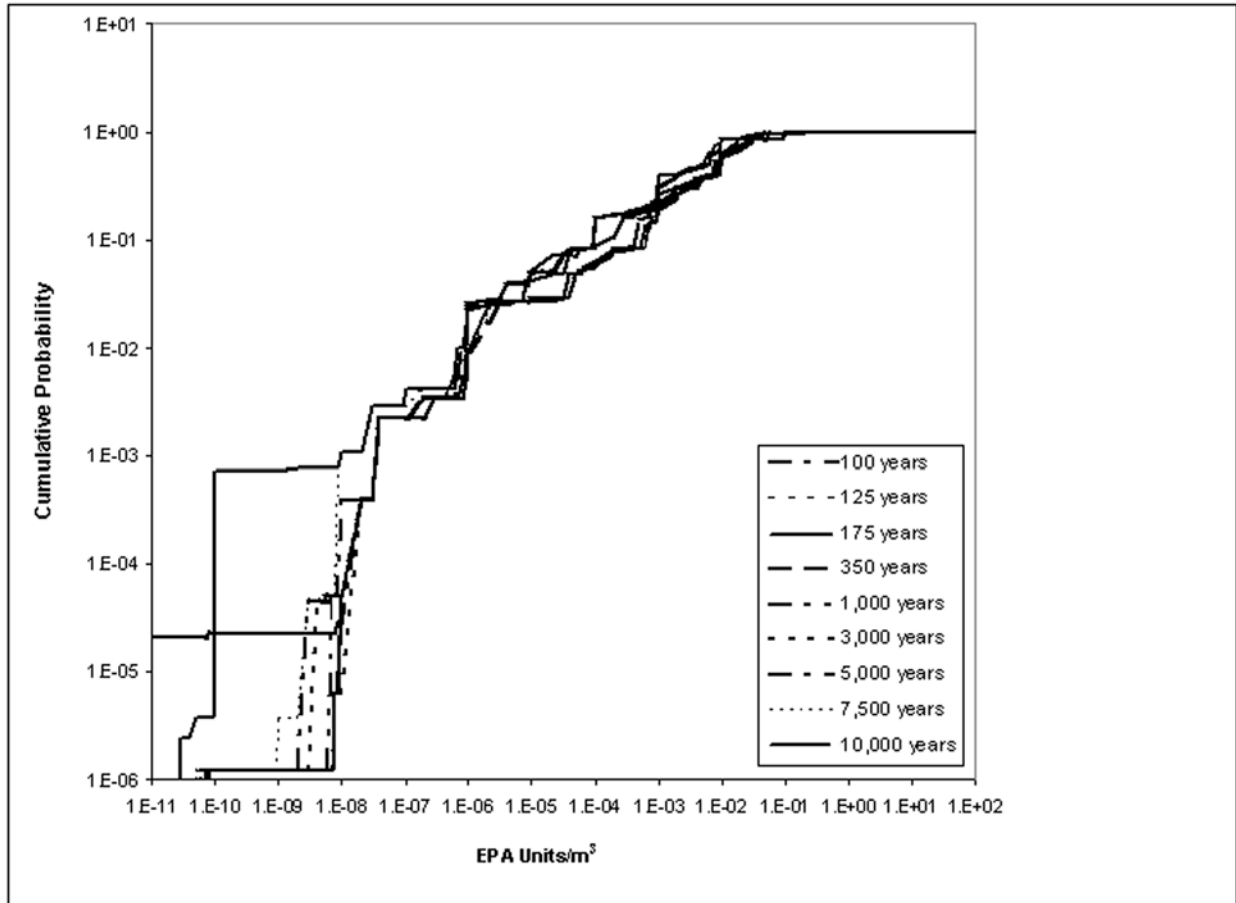
20 For calculation of *To calculate* radionuclide releases from groundwater transport (including
 21 direct brine release) and from spallings, spatial variability in the activity in the waste *activity* is
 22 assumed to have no significant impact. Concentrations of radionuclides mobilized in repository
 23 brine and quantities transported to the ground surface in spallings are assumed to be derived
 24 from a sufficiently large volume of waste that container-scale variability can be neglected. For
 25 *Long-term releases and direct brine releases, releases* are calculated using WIPP-scale data
 26 assuming homogeneous accessibility of RH- and CH-TRU waste activities by liquid in the
 27 repository. As discussed previously, spallings releases are not calculated for RH-TRU waste;



CCA-121-2

1
2
3

Figure 6-296-30. Flowchart Showing Integration of TWBID Data in performance assessment PA Calculations



1
2 **Figure 6-306-31. Cumulative Distribution Function for Waste Stream EPA Units/Volume**

3 consequently, for spallings releases activities are determined assuming homogeneous
4 accessibility for only CH-TRU waste.

5 Direct releases caused by the mechanisms of cuttings and cavings access discrete and relatively
6 small portions of the waste, and estimates of the quantity of radioactivity released to the
7 accessible environment from these mechanisms may be sensitive to variability in activity
8 loading. The radioactivity of cuttings and cavings releases is calculated using data from the
9 waste-stream level in the following manner.

10 Containers are assumed to be *randomly* placed in the WIPP from the various waste streams (*see*
11 *Appendix PA, Attachment MASS, Section 21*) in a random manner. Because waste containers
12 are to be stacked three-high for disposal, a drill bit is assumed to penetrate three containers. The
13 direct-release consequence resulting from a drill bit hitting the edges of containers and
14 generating releases from more than three containers is assumed to be similar to the consequence
15 of penetrating three containers only (*see Appendix PA, Section PA-6.8.3*). Each of the three
16 containers penetrated by the drill bit can come from different waste streams and have different
17 associated activities with them. The waste streams penetrated are randomly sampled according
18 to the relative quantity of waste in each waste stream. Figure 6-31 *Figure 6-30* shows the
19 discretized activities, expressed as the EPA normalized release density, of the 693 569 CH-TRU

1 waste streams as a CDF and the decay of the waste stream activities through time. Waste stream
 2 activities are maintained in ~~performance assessment~~ **PA** at 100, 125, 175, 350, 1,000, 3,000,
 3 5,000, 7,500, and 10,000 years. Activities for cuttings and cavings releases at other times are
 4 interpolated from these values.

5 The code CUTTINGS_S calculates the volume of repository material brought to the surface by
 6 ~~the mechanisms of cuttings and cavings~~. Of the ~~volume of repository~~ **volume** removed,
 7 approximately 40 percent is waste material; the rest is void space, **MgO** (backfill), and drum
 8 packing material. It is assumed that one-third of the waste material released comes from each of
 9 three containers assumed to be intersected. The activity of the release to the surface during
 10 drilling by cuttings and cavings is ~~determined as the summed~~ **of the products** of one-third the
 11 release volume times the three waste stream activities randomly sampled ~~to be intersected~~. If
 12 random sampling determines that the borehole penetrates RH-TRU waste, 100 percent of the
 13 material removed is assumed to be waste and the activity of the release is equal to the volume
 14 calculated by CUTTINGS_S times the activity of RH-TRU waste.

15 6.4.12.5 Diameter of the Intrusion Borehole

16 Historical Delaware Basin drilling records were reviewed to determine the diameter of a typical
 17 intrusion borehole. In ~~performance assessment~~ **PA**, the borehole diameter parameter value is held
 18 constant for all future drilling and is equal to 0.311 m (12.25 in.). Appendix **DATA, Attachment**
 19 **A and CCA Appendix DEL, (DEL Attachment 1)** discusses **current and historical** typical drill
 20 stem and drill collar diameters used to drill oil and gas wells in the Delaware Basin. **CCA**
 21 Appendix DEL (~~Section DEL.6.1.2.2~~) illustrates a generalized circular cross section of a well
 22 plugged according to current practice (~~see Appendix DEL, DEL Attachment 7~~). (**see CCA**
 23 **Section DEL.6.1.2.2l and Appendix DATA**).

24 6.4.12.6 Probability of Intersecting a Brine Reservoir

25 As **discussed** ~~mentioned~~ in Section 6.4.8, there is uncertainty about the existence of brine
 26 reservoirs and ~~uncertainty in~~ the probability of intersecting a brine reservoir with a deep
 27 borehole. The DOE has examined available data and concluded that there is no reasonable basis
 28 to eliminate the possibility of a brine reservoir existing under the site. Therefore, the DOE
 29 assumes that a brine reservoir may exist under the waste panels. The DOE ~~has determined the~~
 30 ~~that there is~~ a reasonable basis for ~~determining~~ the probability of intersecting a brine reservoir
 31 and ~~has~~ pursued three ~~types of investigations~~ relevant to this issue: geophysical methods,
 32 geological structure analysis, and geostatistical correlation. (**see CCA Section 6.4.8, Appendix**
 33 **MASS Section 18, and MASS Attachments 18-1, 2 and 3 for the investigations that led to the**
 34 **CCA's representation of the brine reservoir**). **As discussed in Section 6.4.8, the DOE adopted**
 35 **the EPA's representation of the brine reservoir used in the 1997 PAVT (the EPA's basis for**
 36 **this representation is documented in the Technical Support Document for Section 194.23:**
 37 **Parameter Justification Report, A-93-02, V-B-14 and in a technical support document entitled**
 38 **Technical Report Review of TDEM Analysis of WIPP Brine Pockets, A-93-02, V-B-30).**

39 In 1987, the DOE conducted a series of 38 time-domain electromagnetic (TDEM) soundings at
 40 the WIPP site (Earth Technology Corporation 1988; Appendix MASS, Section MASS.18.1 and
 41 MASS Attachment 18-5). Thirty six of these soundings were executed over a 1 by 2 kilometer

1 area, with the north-central nine soundings located directly over the waste panels. The
2 electromagnetic data collected by the measurements indicate differences in electrical resistivity,
3 which can be interpreted as occurring in the Castile. Regions of relatively low resistivity in the
4 Castile are presumed to be so because of a greater abundance of interconnected brine compared
5 to higher resistivity regions. A sounding executed near the brine reservoir penetrated at WIPP-
6 12 provides an independent calibration on the interpretation of the data. The study indicates the
7 presence of electrically conductive regions below the waste panels at the WIPP. However,
8 because of the inherent coarse resolution of the method, the data do not support the development
9 of a unique map of the extent of conductors in the Castile. A recent interpretation of the data
10 included in Appendix MASS (Section MASS.18.1 and MASS Attachment 18-5) suggests that
11 between 10 percent and 55 percent of the waste panel area may be underlain by relatively
12 conductive units, interpreted to be one or several brine reservoirs. The TDEM data do support a
13 limited probability of intersecting brine. Because of the spatial resolution provided by TDEM
14 data, however, the data do not support distinguishing boundaries between reservoir and
15 nonreservoir areas. Thus, the DOE assumes that one reservoir exists below the waste panels.
16 The geological structure of selected units within the Castile and Salado has been mapped
17 recently to examine more closely the relationship between identified brine intercepts and
18 evaporite deformation. This study is described in Appendix MASS (Section MASS.18.1 and
19 MASS Attachment 18-6). After ERDA-6 encountered brine in steeply dipping beds, studies
20 indicated that many of the other observed brine encounters in the Delaware Basin are associated
21 with structural deformation in the Castile. The study of structure reaffirms the concept that much
22 of the Castile underlying the present WIPP site is generally unreformed. The DOE does not use
23 the results of the structural study in quantifying the existence or probability of intersecting a
24 brine reservoir.

25 The geostatistical study discussed in Appendix MASS (Section MASS.18 and included as MASS
26 Attachment 18-6), was conducted using existing borehole data to estimate the probability of
27 drilling into a fractured reservoir in areas overlain by WIPP underground workings. The
28 database consists of boreholes in the general area of the WIPP where Castile brine has been
29 encountered as well as a much larger number of boreholes in which brine is not reported to have
30 been encountered. The study used geostatistical methods to estimate the probabilities that a
31 randomly placed borehole would encounter pressurized brine in the Castile. These methods do
32 not require assumptions about the distribution of brine reservoirs but are based on the empirical
33 evidence available. Based on geostatistical analysis, the DOE uses a 0.08 probability that any
34 deep borehole drilled within the waste panel penetrates the brine reservoir that is assumed to
35 exist below the waste panels.

36 The *For the CRA-2004 PA*, the DOE assumes that there is one reservoir under the quadrilateral
37 area enclosing the waste panels with *and uses probability of a deep borehole hitting the*
38 *reservoir of between 0.01 to 0.60 (see EPA 1998, VII.B.4.d).* any deep borehole penetrating it.
39 The location of boreholes in this area is sampled. They may lie over repository excavations, or
40 over rock in pillar cores, or between panels. The brine reservoir under the waste panels *is not*
41 *assumed to* can be depleted during the 10,000-year regulatory period by *subsequent* boreholes
42 drilled anywhere within this area. Boreholes that are randomly located over rock have the same
43 probability of intersecting the brine reservoir as boreholes located over excavations. Boreholes
44 located over the excavations are assumed to penetrate waste, and the consequences are modeled
45 as described throughout *in* Section 6.4. Boreholes located over the intact rock in this area are

1 ~~assumed to have no consequences on the disposal system other than that they can contribute to~~
2 ~~the depletion of reservoirs, as discussed below. Long term depletion of pressure and the~~
3 ~~production of brine from a reservoir that may exist under the repository occurs only for the two-~~
4 ~~plug configuration boreholes. Long term depletion does not occur during the 10,000 year~~
5 ~~regulatory period for the solid concrete plug boreholes or three plug configuration borehole.~~

6 BRAGFLO calculates the long-term depletion of pressure and production of brine from the
7 reservoir for only one two-plug configuration borehole. ~~For estimating the consequences of~~
8 ~~possible sequences of future events, the DOE assumes how the reservoir responds to additional~~
9 ~~penetrations. Subsequent penetrations are assumed to behave identically to the first (see~~
10 ~~Appendix PA, Section PA-6.8). until the reservoir is assumed to be completely depleted and~~
11 ~~cannot produce more brine (see Appendix MASS, Section MASS.18 and MASS Attachment 18-~~
12 ~~3). The DOE assumes the 32,000 cubic meter reservoir is depleted after two penetrations; the~~
13 ~~64,000 cubic meter reservoir after four penetrations; the 96,000 cubic meter reservoir after six~~
14 ~~penetrations; the 128,000 cubic meter reservoir after eight penetrations; and the 160,000 cubic-~~
15 ~~meter reservoir after 10 penetrations. Because it is assumed for modeling simplicity that~~
16 ~~penetrations before depletion behave identically to the first penetration, it is possible for a~~
17 ~~reservoir to cumulatively produce more brine with multiple intrusions than it is assumed to~~
18 ~~contain for the first intrusion.~~

19 6.4.12.7 Plug Configuration in the Abandoned Intrusion Borehole

20 As stated in Section 6.4.7, three different plug configurations can ~~be used to represent possible~~
21 ~~future configurations of plugged and abandoned intrusion boreholes. Based on a survey of~~
22 ~~current practice (see Appendix PA, Attachment MASS, Section 16.0 Appendix MASS, Section~~
23 ~~MASS.16.3 and MASS Attachment 16-1), the two-plug configuration borehole is considered~~
24 ~~most likely and is assigned a probability of 0.6968. The three-plug configuration is considered~~
25 ~~less likely and is assigned a probability of 0.28930. The continuous concrete plug is considered~~
26 ~~least likely and is assigned a probability of 0.0152 (SNL 2003).~~

27 6.4.12.8 Probability of Mining Occurring within the Land Withdrawal Area

28 The EPA has specified the probability of mining in the future. In 40 CFR § 194.32 (b), the EPA
29 states, "Mining shall be assumed to occur with a one in 100 probability in each century of the
30 regulatory time frame."

31 Also in 40 CFR § 194.32(b), the EPA limits the occurrence of mining to a maximum of once per
32 10,000 years. The DOE ~~has interpreted this probability model as a Poisson model with a of~~
33 ~~mining probability of 10^{-4} per year (Appendix PA, CCDFGE, Section PA-3.0). During the~~
34 ~~period that passive institutional controls are effective, the probability of mining is 10⁻⁶ per year.~~
35 The occurrence of mining is sampled from a CDF of the time until mining in a manner similar to
36 the procedure described for the time between drilling intrusions, except that multiple mining
37 events cannot occur.